Since January 2020 Elsevier has created a COVID-19 resource centre with free information in English and Mandarin on the novel coronavirus COVID-19. The COVID-19 resource centre is hosted on Elsevier Connect, the company's public news and information website.

Biochimica et Biophysica Acta 1778 (2008) 1407–1414

Contents lists available at ScienceDirect

Biochimica et Biophysica Acta

journal homepage: www.elsevier.com/locate/bbamem

N-linked glycosylation and its impact on the electrophoretic mobility and function of the human proton-coupled folate transporter (*Hs*PCFT)☆

Ersin Selcuk Unal [b], Rongbao Zhao [a,b], Andong Qiu [a,b], I. David Goldman [a,b,*]

[a] Department of Medicine, Albert Einstein College of Medicine, 1300 Morris Park Avenue, Bronx, NY 10461, USA
[b] Department of Molecular Pharmacology, Albert Einstein College of Medicine, 1300 Morris Park Avenue, Bronx, NY 10461, USA

ARTICLE INFO

Article history:
Received 19 September 2007
Received in revised form 7 March 2008
Accepted 7 March 2008
Available online 20 March 2008

Keywords:
PCFT, proton-coupled folate transporter
HCP1
PCFT/HCP1
PCFT glycosylation
Folate transport
Intestinal folate absorption
PCFT secondary structure
Hereditary folate malabsorption (HFM)
SLC46A1

ABSTRACT

The human proton-coupled folate transporter (*Hs*PCFT, SLC46A1) mediates intestinal absorption of folates and transport of folates into the liver, brain and other tissues. On Western blot, *Hs*PCFT migrates as a broad band (~55 kDa), higher than predicted (~50 kDa) in cell lines. Western blot analysis required that membrane preparations not be incubated in the loading buffer above 50 °C to avoid aggregation of the protein. Treatment of membrane fractions from *Hs*PCFT-transfected HeLa cells with peptidyl *N*-glycanase F, or cells with tunicamycin, resulted in conversion to a ~35 kDa species. Substitution of asparagine residues of two canonical glycosylation sites to glutamine, individually, yielded a ~47 kDa protein; substitution of both sites gave a smaller (~35 kDa) protein. Single mutants retained full transport activity; the double mutant retained a majority of activity. Transport function and molecular size were unchanged when the double mutant was hemagglutinin (HA) tagged at either the NH_2 or COOH terminus and probed with an anti-HA antibody excluding degradation of the deglycosylated protein. Wild-type or deglycosylated *Hs*PCFT HA, tagged at amino or carboxyl termini, could only be visualized on the plasma membrane when HeLa cells were first permeabilized, consistent with the intracellular location of these domains.

1. Introduction

Mammals meet their biosynthetic needs for one carbon donors by absorbing dietary folates in the acidic microclimate at the brush-border membrane of the upper small intestine [1]. Polyglutamate derivatives of 5-methyltetrahydrofolate constitute more than 90% of folate nutrients [2]. Prior to absorption, these congeners are hydrolyzed by gamma-carboxypeptidase to the monoglutamate which is the major blood folate [3]. Until recently, the reduced folate carrier (RFC, SLC19A1), which is expressed at the apical brush-border membrane along the entire intestine [4,5], was considered to represent the mechanism by which folates are absorbed [6] despite the fact that the absorptive mechanism was known to have a different pH optimum and structural specificity [7]. Recently, a novel folate transporter (PCFT) was identified that recapitulates the properties of intestinal folate absorption [8]. Confirmation that this transporter is required for intestinal folate absorption came from the observation that loss-of-function mutations in *Hs*PCFT are the genetic basis for hereditary folate malabsorption (HFM) (OMIM 229050) [8,9], an autosomal recessive disorder characterized by defects in both intestinal folate absorption and folate transport into the central nervous system [10].

Besides the small intestine, *Hs*PCFT mRNA is expressed in kidney, liver, placenta, and to a lesser extent in other tissues [8]. Likewise, a low-pH folate transport activity, now attributed to PCFT, has been demonstrated in the intestine [1,11], liver [12], kidney [13], and in human solid tumor cell lines [14,15]. *Hs*PCFT mediated folate transport can be distinguished from RFC mediated transport: (i) the former has a low-pH optimum (~5.5) while RFC has a pH optima of ~7.4. (ii) *Hs*PCFT has a high affinity for folic acid and other folates (K_m's range from 0.5 to 1 μM) at low pH which decreases as the pH is increased. RFC has a very low affinity for folic acid (K_i ~200 μM) which, along with its affinity for other folates/antifolates, is largely pH-independent over a pH range of 5.5 to 7.4 [16]. RFC has a very high affinity (K_i ~0.2 μM) for PT523; *Hs*PCFT has a very low affinity (>50 μM) for this antifolate [8,17].

*Hs*PCFT protein has been detected at different molecular sizes in cell lines and species, attributed to post-translational modification, most likely by N-linked glycosylation [8]. Although the Asn-Xaa-Ser/Thr signals or sequons are present in the *Hs*PCFT sequence (N58, N68), not all sequons are glycosylated due either to the effects of neighboring amino acid residues or their intra- versus extracellular

☆ Data in this paper are from Ersin S. Unal's thesis to be submitted in partial fulfillment of the requirements for the Degree of Doctor of Philosophy in the Graduate Division of Medical Sciences, Albert Einstein College of Medicine, Yeshiva University. This work was supported by a grant from the National Institutes of Health (CA-082621).

* Corresponding author. Cancer Center, Albert Einstein College of Medicine, 1300 Morris Park Avenue, Bronx, NY 10461, USA.
E-mail address: igoldman@aecom.yu.edu (I.D. Goldman).

Abbreviations: RFC, reduced folate carrier; PCFT, proton-coupled folate transporter; SLC, solute carrier family; TMDs, transmembrane domains; PNGaseF, peptide-N^4-(*N*-acetyl-β-D-glucosaminyl)asparagine amidase F; Endo H, endo-β-*N*-acetylglucosaminidase H; MTX, methotrexate; DTT, dithiothreitol; SDS-PAGE, sodium dodecyl sulfate polyacrylamide gel electrophoresis; OMIM, Online Mendelian Inheritance in Man

0005-2736/$ – see front matter © 2008 Elsevier B.V. All rights reserved.
doi:10.1016/j.bbamem.2008.03.009

locations [18,19]. This study was designed to determine the extent to which *Hs*PCFT is, in fact, glycosylated and the impact of glycosylation on the electrophoretic properties of the protein and its transport function.

2. Materials and methods

2.1. Chemicals

Tritiated methotrexate (MTX-disodium salt, [3′, 5′, 7-[^{3}H](N)]) (Catalog number MT701) was obtained from Moravek Biochemicals Inc. (Brea, CA), purified by liquid chromatography, and maintained as previously described [20]. PNGaseF (peptide-N^4-(*N*-acetyl-β-D-glucosaminyl)asparagine amidase F) (G5166) and tunicamycin from Streptomyces species (T7765) were obtained from Sigma (St. Louis, MI). Protease inhibitor cocktail (Cat# 11836170001) was obtained from Roche Applied Science (Mannheim, Germany).

2.2. Site-directed mutagenesis

Site-directed mutagenesis was carried out according to the QuikChange II XL protocol from Strategene (La Jolla, CA). Wild-type *Hs*PCFT cDNA cloned into the *Bam*HI site of the mammalian expression vector pcDNA3.1(+) was used as the template [8]. Two complementary forward and reverse primers, which carry the targeted nucleotide changes in the middle region, were designed individually for introducing glutamines into *Hs*PCFT primary sequence at positions 58, 68 and 58/68 [Table 1]. After initial denaturation at 95 °C for 1 min, the targeted vectors were generated for 18 cycles of 50 s at 95 °C for denaturation, 50 s at 60 °C for annealing, 16 min at 68 °C for extension followed by a final extension period of 7 min at 68 °C. *Dpn*I (10 U/μL) restriction enzyme was used to digest the parental dsDNA. The mixture (3 μL) was transformed into Top10 ultra competent cells (Invitrogen). Plasmids carrying the desired mutations were identified by DNA automated sequencing in the Albert Einstein Cancer Center Genomics Shared Resource. The entire coding region of *Hs*PCFT was sequenced to confirm the absence of any other polymerase introduced mutations.

2.3. Epitope tagging

A hemagglutinin (HA) peptide epitope (YPYDVPDYA) was fused to the wild-type and N58Q/N58Q-*Hs*PCFT by PCR-based site-directed mutagenesis using the primers listed in Table 1. A *Bgl*II restriction site was included in the upstream N-terminal HA tag primer sequence for subcloning. The PCR product was purified, digested with *Bgl*II, and ligated into *Bam*HI-digested *Hs*PCFT in pcDNA3.1(−) to generate the N-HA-*Hs*PCFT and N-HA-N58Q/N68Q-*Hs*PCFT. The downstream primer used for introducing the C-terminal HA epitope contained an *Xba*I restriction site. The upstream primer included a *Hind*III restriction site. The PCR product was purified, digested with *Hind*III and *Xba*I, and ligated into *Hind*III–*Xba*I digested *Hs*PCFT in pcDNA3.1(+) to generate the C-HA-*Hs*PCFT and C-HA-N58Q/N68Q-*Hs*PCFT. The ligation products were transformed into Top10 ultra competent cells (Invitrogen). Plasmids carrying the HA tags were identified by DNA automated sequencing.

2.4. Cell culture and transfection

HeLa cells, originally obtained from the American Type Tissue Collection (Manassas, VA), have been maintained in this laboratory in RPMI-1640 medium supplemented with 10% fetal bovine serum, 100 U/mL penicillin and 100 μg/mL streptomycin at 37 °C in a humidified atmosphere of 5% CO_2. Lipofectamine 2000 (Invitrogen) was used according to the manufacturer's protocol for transient transfection of plasmid DNA into these cells. To create stably transfected HeLa cell lines, transiently transfected cells were trypsinized and passaged into 100 mm culture plates at appropriate densities and allowed to grow in RPMI-1640 media containing 800 μg/mL of G418 sulfate (Mediatech, Herndon, VA). Individual clones were isolated, expanded and maintained in the same medium supplemented with 800 μg/mL of G418. Several (>20) clones expressing the desired N- and C-terminus tagged wild-type and N58Q/N68Q-*Hs*PCFT were screened and one clone of each construct with the highest activity was selected for further analysis. HeLa cells were transfected with empty pcDNA3.1(+) vector (mock) or the same vector containing wild-type or mutant HsPCFT. [^{3}H]MTX influx was then assessed at pH 5.5.

Table 1
Primers for site-directed mutagenesis and PCR primers for N- and C-terminal HA-epitope insertions for wild-type and N58Q/N68Q-*Hs*PCFT

		Primer sequence (5′ to 3′)
N58Q	Forward	GCCGACCTCGGCTACCAAGGCACCCGCCAAAGG
	Reverse	CCTTTGGCGGGTGCCTTGGTAGCCGAGGTCGGC
N68Q	Forward	AGGGGGGGCTGCAGCCAACGCAGCGCGGACCCC
	Reverse	GGGGTCCGCGCTGCGTTGGCTGCAGCCCCCCCT
N58Q/N68Q	Forward	GCCGACCTCGGCTACCAAGGCACCCGCCAAA
		GGGGGGGCTGCAGCCAACGCAGCGCGGACCCC
	Reverse	GGGGTCCGCGCTGCGTTGGCTGCAGCCCCC
		CCTTTGGCGGGTGCCTTGGTAGCCGAGGTCGGC
N-terminal HA tag	Forward	TCAAGATCTCACCATGTACCCATACGATGTTCCA
		GATTACGCTATGGAGGGGCGCGTGAGC
	Reverse	TATAGATCTCAGGGGCTCTGGGGAAACTG
C-terminal HA tag	Forward	TATAAGCTTCACCATGGAGGGGAGCGCGAGC
	Reverse	TCATCTAGATTAAGCGTAATCTGGAACATCG
		TATGGGTAGGGCTCTGGGGAAACTG

2.5. PNGaseF and EndoH treatment

Enzymatic deglycosylation of total membrane protein (200 μg) prepared (see Western blot analysis below) from *Hs*PCFT cDNA-transfected HeLa cells was performed with PNGaseF enzyme (Sigma, G5166) following the manufacturer's protocol. Because heat denaturation was omitted, the incubation time of the protein sample in 250 mM phosphate buffer (pH 7.5) and 2.5 μL of 2% SDS with 1 M 2-mercaptoethanol was increased to 1 h at room temperature. Cleavage of the asparagine-*N*-acetyl glucosamine bond was monitored by SDS-PAGE. Membrane preparations were treated with EndoH (Roche Diagnostics, Mannheim, Germany) following the manufacturer's protocol. RNaseB (New England Biolabs) was treated under the same conditions as a control for EndoH activity.

2.6. Tunicamycin treatment

Tunicamycin (T7765)(Sigma, St. Louis, MI) was dissolved in DMSO and added to growth medium to achieve concentrations of 0.25, 0.5, 1 μg/mL at the same time the cells were transfected with *Hs*PCFT cDNA. Tunicamycin remained in the growth medium for 48 h when the cells were assayed.

2.7. Membrane transport measurements

Cells were seeded in 17 mm glass scintillation vials to a final density of 4×10^5 cells/mL. When cells reached mid-log phase growth ~72 h later, as determined microscopically, uptake determinations were performed [21]. Briefly, the media was aspirated and the cells incubated with HEPES Buffered Saline (HBS) (20 mM HEPES, 5 mM dextrose, 140 mM NaCl, 5 mM KCl, 2 mM $MgCl_2$, at pH 7.4) for 20 min. To initiate uptake, HBS was removed, MES buffered saline (MBS) (20 mM MES, 140 mM NaCl, 5 mM KCl, 2 mM $MgCl_2$, 5 mM dextrose, at pH 5.5) containing [^{3}H]MTX (0.5 μM, specific activity 1000–2000 dpm/pmol) was added to the cells. Uptake was stopped by placing the vial in ice followed by rapid but careful addition of 6 mL of ice-cold HBS (pH 7.4). After three washes, cells were lysed with 0.5 mL of 0.2 N NaOH at 65 °C for 30 min; 400 μL of lysate was used to determine radioactivity in a liquid scintillation spectrometer. Total protein for each sample was determined on a 20 μL portion of the lysate by the BCA protein assay reagent kit (Pierce, Rockford, IL). Data is expressed as pmol MTX/vial and normalized to total protein (pmol/mg protein).

2.8. Western blot analysis

Confluent HeLa cells in 17-mm glass scintillation vials were washed twice with ice-cold PBS and the cells were scraped off with PBS containing Roche protease inhibitor. To obtain total membrane fractions, cells were incubated on ice for 30 min in hypotonic buffer (200 μL/10^6 cells) (0.5 mM Na_2HPO_4, 0.1 mM EDTA at pH 7.4) containing protease inhibitor, following which the membrane fraction was pelleted by centrifugation at 14,000 ×*g* and 4 °C for 2 min. The pellet was resuspended in lysis buffer (100 μL/10^6 cells; 20 mM TRIS-base, 150 mM NaCl, 1% Triton X-100, 0.1% SDS, 1 mM EDTA at pH 7.4) and briefly sonicated with the Microson XL 2000 ultrasonic liquid processor (Misonix Incorporated, Farmingdale, NY) and protein was determined as indicated above. Proteins were dissolved in SDS-PAGE loading buffer (0.225 M Tris.Cl [pH 6.8], 50% glycerol, 5% SDS, 0.05% bromphenol blue) with or without 0.25 M dithiothreitol (DTT). Portions of the preparation were then subjected to a 10 min incubation at room temperature, 50 °C, 75 °C or 95 °C following which proteins were resolved on a 12% SDS-polyacrylamide gel. The proteins were then transferred to PVDF Transfer Membranes (Amersham Life Science). A polyclonal anti-*Hs*PCFT antibody to the distal C-terminus of *Hs*PCFT (amino acids 446–459) was used to probe the plasma membrane as previously described [8]. A rabbit anti-HA antibody (#H6908) obtained from Sigma (St. Louis, MI) was used to detect HA-tagged proteins. Membranes were processed by the ECL Plus Western Blotting Detection System (Amersham Life Science).

2.9. Immunofluorescence microscopy

A commercially available Alexa Fluor 488 conjugated anti-HA monoclonal antibody 16B12 (1 mg/mL) obtained from Invitrogen (Carsbad, CA) was used to localize HA-tagged wild-type and N58Q/N68Q-*Hs*PCFT proteins by direct immunofluorescence. Stably transfected HeLa cells grown on coverslips were washed five times with RPMI-1640 medium and the cells fixed with 1% paraformaldehyde for 30 min at room temperature. Cells were permeabilized with 0.2% Triton X-100 in PBS for 15 min at RT. The cells were blocked with 2% bovine serum albumin containing 5% donkey serum (blocking buffer) for 30 min, then 200 μL of Alexa Fluor 488 conjugated anti-HA monoclonal antibody solution (1 μL of antibody in 8 mL of blocking buffer) was added to

each coverslip. After 1 h at room temperature, cells were washed 10 times with PBS, each for 5 min, and coverslips were placed on slides with mounting medium containing propidium iodide to visualize DNA (Vector, CA). The slides were then sealed and viewed with an Olympus IX70 Inverted Epifluorescence Microscope (Center Valley, PA) with 488 nm excitation.

2.10. Data analysis

Data presented is the mean ± standard error of the mean (SEM) of at least three independent experiments. Statistical comparisons were performed by the two-tailed Student's paired *t*-test. Some experiments were assessed using a one-way repeated measures analysis of variance (ANOVA) and the Tukey's post test. All statistical analyses were performed using GraphPad PRISM (version 3.0 for Windows, GraphPad Software).

3. Results

3.1. Computational analysis of the HsPCFT protein sequence

*Hs*PCFT protein (NP_542400) consists of 459 amino acids with a predicted molecular weight (MW) of ~50 kDa (http://ca.expasy.org/tools/protparam.html). *Hs*PCFT is a basic protein, with a predicted pI of 9.03, highly enriched with hydrophobic residues. The primary structure of the protein has two putative N-linked glycosylation consensus sites (http://www.cbs.dtu.dk/services/NetNGlyc) at positions Asn^{58} (N-G-T) and Asn^{68} (N-R-S), as illustrated in Fig. 1. These sites are predicted to be within the extracellular loop between TMDs I and II (HMMTOP, PredictProtein, TMpred, TopPred analyses). The glycosylation consensus sites (N-X-S/T) are highly conserved among species [*Macaca mulatta* (XP_001106954), *Mus musculus* (NP_081016), *Bos taurus* (NP_001073053), *Xenopus laevis* (AAH77859), *Danio rerio* (NP_956579), *Monodelphis domestica* (XP_001375817), *Rattus norvegicus* (NP_001013991), *Canis familiaris* (XP_548286)] (http://www.ebi.ac.uk/clustalw/).

3.2. The effect of temperature on HsPCFT protein stability

When membrane samples were heated for 5–20 min at 95 °C to denature the protein in preparation for SDS-PAGE, as is the conventional method [22–24], no protein was detected likely due to HsPCFT aggregation and immobilization in the stacking gel. To establish conditions that obviate aggregation, plasma membrane protein fractions were prepared from HeLa cells 48 h after transfection with *Hs*PCFT cDNA, then incubated in the loading buffer containing SDS with and without DTT at RT, 50 °C, 75 °C or 95 °C for 10 min before PAGE. When incubated in SDS solution at RT or 50 °C, protein migrated as three bands: (i) a broad band centered at ~55 kDa, (ii) a smaller band at ~47.2 kDa, and (iii) the narrowest band at ~35.1 kDa. But there was no detectable protein on the separating gel when it was heated above 50 °C (Fig. 2). *Hs*PCFT protein was detected in stacking gels but not the separating gel when the sample was heated at 75 °C and 95 °C (data not shown). Based on these observations, membrane fractions were maintained on ice or room temperature in the loading buffer prior to SDS-PAGE.

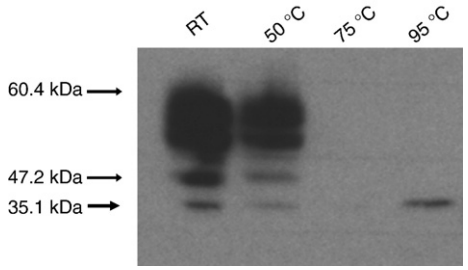

Fig. 2. The effect of heating on Western blot analysis of *Hs*PCFT. Equal amounts of lysate (30 µg) were incubated in the loading buffer with DTT at the indicated temperatures for 10 min before loading onto the SDS-gel. The blots were probed with a polyclonal peptide antibody directed to the C-terminus of *Hs*PCFT. The numbers on the left indicate the molecular sizes of protein bands. The blot is representative of three separate experiments.

3.3. Assessment of N-linked glycosylation with PNGaseF and EndoH

The molecular size of the *Hs*PCFT protein detected in HeLa cells, ~55 kDa, was higher than the predicted molecular weight of ~50 kDa [8]. As indicated above, there are two predicted N-linked glycosylation sites in the first extracellular loop of *Hs*PCFT. To determine if this size discrepancy is due to post-translational glycosylation at these sites, membranes from HeLa cells transiently transfected with *Hs*PCFT

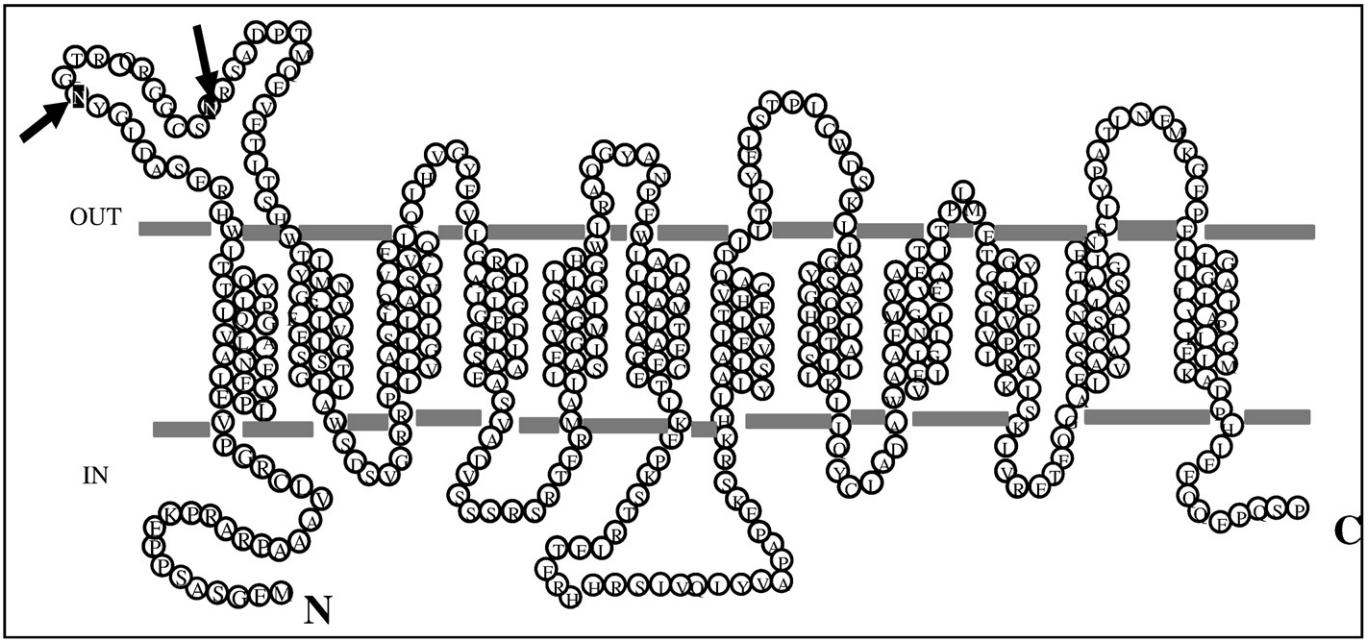

Fig. 1. A membrane topology model for *Hs*PCFT predicted by online databases (http://www.expasy.org/tools/#topology) and the locations of asparagine residues in the N-linked glycosylation consensus sites (arrows).

cDNA were treated with PNGaseF, which cleaves the bond between the first *N*-acetyl glucosamine of both complex and high mannose oligosaccharides and the asparagine residue in the canonical consensus sequence [25]. Untreated protein displayed the above-noted three bands: a broad band centered at ~55 kDa and two other smaller bands detected at ~47.2 kDa and ~35.1 kDa. When protein samples were treated with PNGaseF, virtually all protein migrated at a molecular weight of ~35.1 kDa with only very low levels of higher MW bands that likely represent incomplete PNGaseF reaction products (Fig. 3). Membrane protein fractions of HeLa cells transiently transfected with *Hs*PCFT were also treated with EndoH [26]. There was no detectable change in the Western blot. This was unlike the results with RNaseB, an established substrate for EndoH, in which there was an expected gel-shift upon similar treatment with this enzyme (data not shown).

3.4. Assessment of N-linked glycosylation in intact HeLa cells with tunicamycin

Another approach was utilized to assess glycosylation of *Hs*PCFT based on inhibition of *de novo* N-linked glycosylation by tunicamycin [27]. HeLa cells transiently transfected with *Hs*PCFT cDNA were exposed to a spectrum of tunicamycin concentrations for 48 h following which crude plasma membranes were prepared and subjected to Western blot analysis. As indicated in Fig. 4 (lower panel), high molecular weight *Hs*PCFT bands decrease as the tunicamycin concentration was increased; this was accompanied by an increase in the ~35 kDa band. By 1.0 μg/mL tunicamycin, the only band present was at 35.1 kDa. Studies were also undertaken to determine the impact of tunicamycin inhibition of *Hs*PCFT glycosylation on transport function in HeLa cells. There was no significant effect of low levels of tunicamycin on [^{3}H]MTX influx (Fig. 4, upper panel) and the small decrease (~22%) observed at 1 μM drug, when glycosylation was completely inhibited, was not statistically significant (p=0.09).

3.5. Site-directed mutagenesis of N-linked glycosylation sites

To further verify the N-linked glycosylation sites and their functional importance, three different site-directed mutants of *Hs*PCFT were constructed at the putative *N*-glycosylation sites. The asparagine residues at Asn58 and Asn68 were replaced either singly or together by a glutamine residue to yield the Asn58Gln (N58Q-*Hs*PCFT), Asn68Gln (N68Q-*Hs*PCFT) single mutants and the N58Q/N68Q-*Hs*PCF double mutant. To assess the functional consequences of these mutations, wild-type *Hs*PCFT and the mutant constructs were transiently expressed in HeLa cells and influx of 0.5 μM [^{3}H]MTX was assessed. As shown in Fig. 5 (upper panel), influx in the N58Q-*Hs*PCFT and N68Q-*Hs*PCFT single mutant transfectants was 79–83% of the transport rate detected in wild-type *Hs*PCFT cDNA-transfected cells (p>0.05). [^{3}H]MTX influx was decreased by 40% in the double mutant (p=0.05).

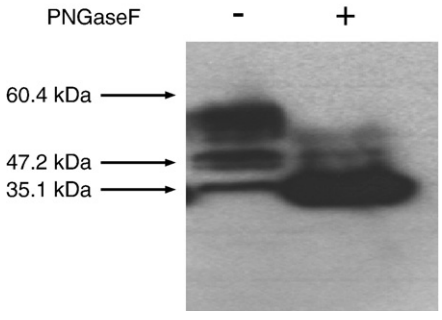

Fig. 3. The effect of PNGaseF treatment on the apparent molecular size of *Hs*PCFT. *In vitro* enzymatic deglycosylation was achieved by addition of PNGaseF (10 U/mL) to 200 μg of membrane protein with incubation for 3 h at 37 °C. An equal amount of PNGaseF treated (right lane) and control (left lane) lysate (30 μg) was loaded and the blots were probed with a peptide antibody directed to the C-terminus of *Hs*PCFT. Numbers on the left indicate the molecular sizes in the protein ladders. The blot is representative of three separate experiments.

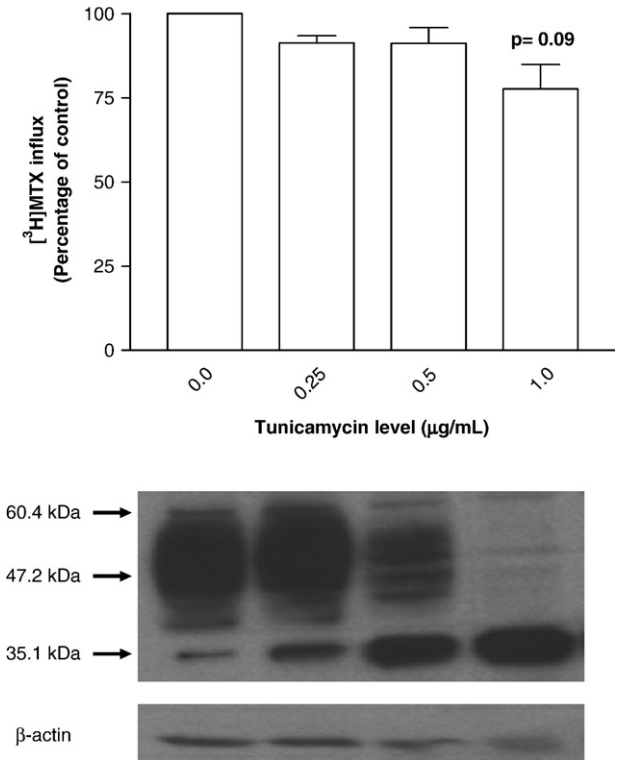

Fig. 4. The effect of tunicamycin treatment on the transport function (upper panel) and the apparent molecular size (lower panel) of *Hs*PCFT. Upper panel; [^{3}H]MTX influx in Hela cells transiently transfected with *Hs*PCFT cDNA and treated with tunicamycin. Uptake of 0.5 μM [^{3}H]MTX was assessed at pH 5.5 and 37 °C over 2 min in HeLa cells grown in the absence or presence of tunicamycin for 48 h. The transport activity in control cells is 214.0±30.2 pmol/mg/2 min. The p value reflects the comparison of the difference between control cells and cells treated with 1 μg/mL tunicamycin. Data are the mean±SEM from three independent experiments. Lower panel; Western blot analysis of *Hs*PCFT protein after tunicamycin treatment of HeLa cells. Equal amounts of lysate (30 μg) from HeLa cells, grown in the presence of increasing tunicamycin concentrations were loaded and the blots were probed with a peptide antibody directed to the C-terminus of *Hs*PCFT. The numbers on the left indicate the molecular sizes in the protein ladders. The blot is representative of three separate experiments.

Immunoblots of the crude plasma membranes prepared from HeLa cells transiently transfected with *Hs*PCFT cDNA, using anti-*Hs*PCFT antibody, showed wild-type *Hs*PCFT protein running at an apparent molecular weight of ~55 kDa, Asn58Gln/Asn68Gln-*Hs*PCFT protein running at a molecular weight of ~35 kDa, and both N58Q-*Hs*PCFT and N68Q-*Hs*PCFT with a predominant band at an apparent molecular weight of ~47 kDa, a size intermediate between that of the wild-type and the double mutant *Hs*PCFT (Fig. 5, lower panel). Hence, both Asn58 and Asn68 residues were glycosylated, and produced a similar alteration in the migration pattern of the protein on SDS-PAGE. These observations confirm that the ~35 kDa band represents deglycosylated *Hs*PCFT.

3.6. Analysis of the structural integrity of C- or N-terminus hemagglutinin (HA) tagged wild-type and deglycosylated (Asn58Gln/Asn68Gln) HsPCFT mutants in HeLa cells

The migration pattern observed by deglycosylation of *Hs*PCFT *in vitro* with PNGaseF, after inhibition of N-linked glycosylation in intact cells with tunicamycin or by site-directed mutagenesis, all

produced a protein with a much lower molecular size than predicted. To evaluate the possibility that this was due to proteolytic degradation, wild-type and N58Q/N68Q-*Hs*PCFT, HA-tagged at either the N- or C-terminus, were transiently transfected into HeLa cells and Western blot analysis was performed with anti-HA antibody. The HA tag at either terminus did not affect the function of the wild-type *Hs*PCFT or the deglycosylated mutant (Fig. 6, upper panel). When probed with anti-HA antibody, both N- or C-terminus HA-tagged wild-type *Hs*PCFT migrated predominantly to a mean molecular size of ~55 kDa with a smaller band at ~47 kDa. Both N- or C-terminal HA-tagged N58Q/N68Q-*Hs*PCFT migrated at a single band at a MW of ~35 kDa (Fig. 6, lower panel). These data exclude proteolytic degradation of wild-type or deglycosylated forms of *Hs*PCFT as a basis for the lower than predicted molecular size observed on Western blot. Hence, the anomalous migration of the *Hs*PCFT protein on SDS-PAGE appears to be an intrinsic characteristic of the protein under these conditions.

3.7. Localization of the wild-type and deglycosylated HsPCFT proteins HA tagged at the amino or carboxyl terminus

Localization of the wild-type and N58Q/N68Q-*Hs*PCFT, stable transfectants with high level expression of either the N- or C-terminus HA-epitope tag was assayed by immunofluorescence staining with or without membrane permeabilization. As indicated in Fig. 7, fluorescence was detected in all permeabilized cells with the exception of mock transfected cells. No fluorescence could be detected in cells that were not permeabilized. Hence, both wild-type and deglycosylated *Hs*PCFT proteins localized to the plasma membrane and both N- and C-termini were accessible to the antibody only when cells were permeabilized under these conditions. These data are consistent with a cytosolic localization for both the N- and C-terminus and indicates that the lack of *N*-glycosylation has little or no effect on *Hs*PCFT membrane targeting.

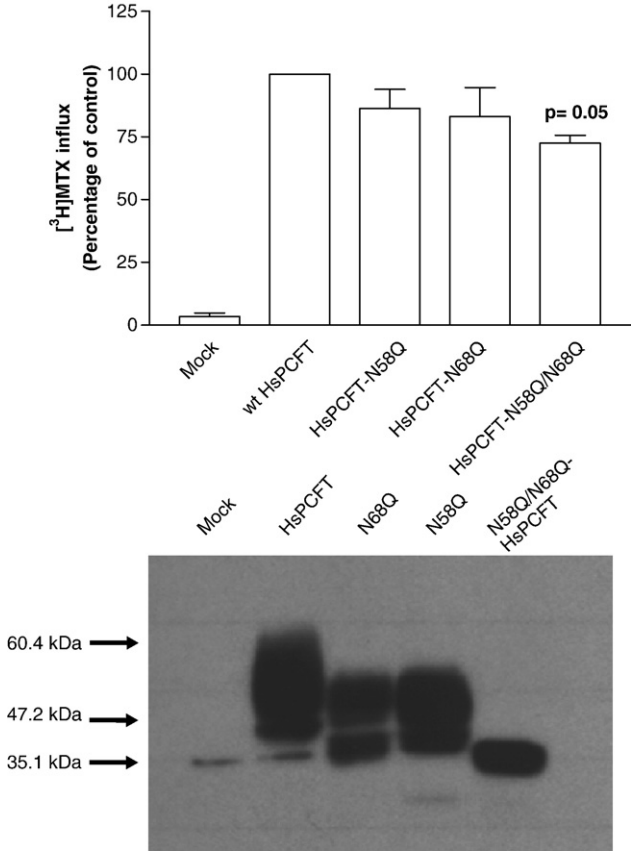

Fig. 5. The transport function (upper panel) and molecular size (lower panel) of N58Q-, N68Q- and N58Q/N68Q-*Hs*PCFT mutants. Upper panel; [^{3}H]MTX influx in HeLa cells transiently transfected with wild-type *Hs*PCFT or glycosylation mutants. Uptake of 0.5 μM [^{3}H]MTX was assessed at pH 5.5 and 37 °C over 2 min. Transport activity in wild-type transfectants is 155.3 ± 36.4 pmol/mg/2 min. The *p* value reflects the difference in activities of the mutant as compared to the wild-type *Hs*PCFT transfectants. Data are the mean ± SEM from three independent experiments. Lower panel; Western blot analysis of wild-type and glycosylation mutant *Hs*PCFT membrane proteins. An equal amount of lysate (20 μg) was loaded and the blots were probed with a peptide antibody directed to the C-terminus of *Hs*PCFT. The numbers shown on the left side indicate the molecular sizes in the protein ladders. The blot is representative of three separate experiments.

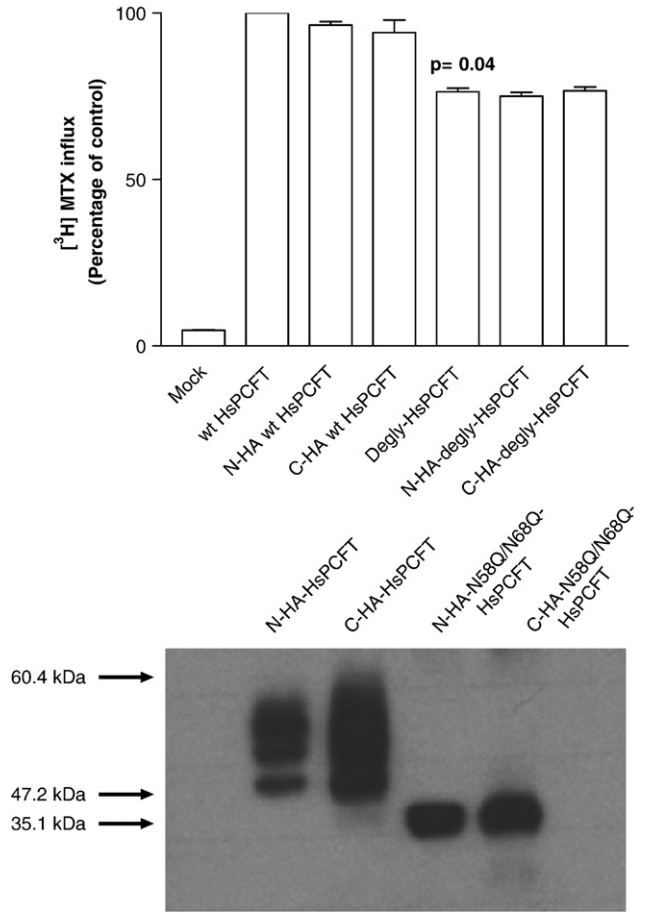

Fig. 6. The effect of HA tagging on the transport function (upper panel) and molecular size (lower panel) of the wild-type and deglycosylated (N58Q/N68Q) *Hs*PCFT. Upper panel; [^{3}H]MTX influx in HeLa cells transiently transfected with cDNAs of N- or C-terminus HA-tagged wild-type and N58Q/N68Q-*Hs*PCFT mutant (degly-*Hs*PCFT). Influx of 0.5 μM [^{3}H]MTX was assessed at pH 5.5 and 37 °C over 2 min. Transport activity in wild-type transfectants is 288.8 ± 12.6 pmol/mg/2 min. The *p* value reflects the difference in activity between the wild-type and deglycosylated *Hs*PCFT. Data are the mean ± SEM from three independent experiments. Lower panel; Western blot analysis of membrane proteins from HeLa cells transiently transfected with wild-type or deglycosylated *Hs*PCFT fused with an HA epitope on either the N- or C-terminus. An equal amount of lysate (20 μg) was loaded and the blots were probed with a monoclonal anti-HA antibody. The numbers on the left indicate the molecular sizes in the protein ladders. Each blot is representative of three separate experiments.

4. Discussion

*Hs*PCFT is a recently discovered carrier protein that mediates intestinal folate absorption and transport of folates into the central nervous system [8]. *Hs*PCFT is expressed in other tissues as well and a low-pH folate transport activity, presumably *Hs*PCFT, is present in most human solid tumors and likely contributes to transport of folates in these settings [8,14]. The murine ortholog of *Hs*PCFT was reported to be a heme carrier protein, (HCP-1, SLC46A1), responsible for intestinal heme absorption that functions independent of pH (over a

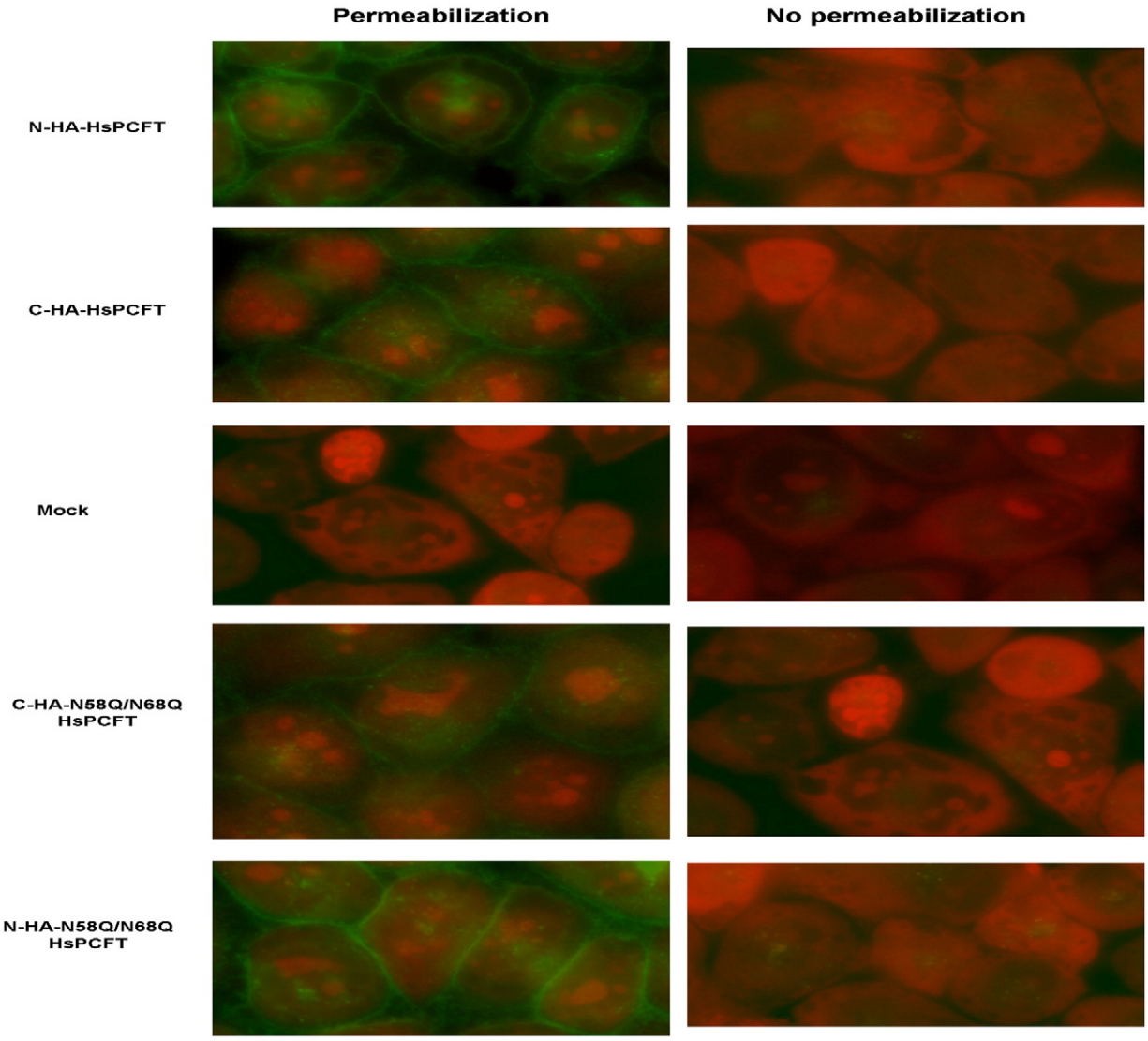

Fig. 7. Immunofluorescence staining of wild-type and deglycosylated *Hs*PCFT. HeLa cells were stably transfected with cDNA of wild-type or deglycosylated *Hs*PCFT fused with the HA epitope on either the N- or C-terminus, then exposed to Alexa Fluor 488 conjugated anti-HA monoclonal antibody. Green fluorescence indicates localization of *Hs*PCFT, while red fluorescence indicates nucleic acids counterstained by propidium iodide. The image is representative of at least three experiments. The left panel shows cells subjected to permeabilization with Triton X-100 before exposure to antibody. The right panel shows cells that were not permeabilized.

pH range of from 6.5 to 8.0) and with a low affinity for heme (K_m=125 μM for [^{55}Fe]hemin) [28]. However, in studies from this laboratory [8], and in a recent report from another laboratory [29], it is clear that this is a high-affinity folate transporter (influx K_m's in the range of 0.2–1.0 μM) with a low-pH optimum. Additional confirmation that the major, if not sole, function of this carrier is folate transport comes from the observation that loss-of-function mutations in *Hs*PCFT result in an autosomal recessive disorder, hereditary folate malabsorption. Individuals with this disorder show no evidence of iron deficiency and the metabolic consequences of the transport defect can be corrected solely by the administration of pharmacological doses of folate [8,9].

The data indicate that *Hs*PCFT is highly heat labile; at temperatures above 50 °C the protein aggregates, a condition that must be considered in the preparation of cell membranes for SDS-PAGE. The basis for this aggregation is not clear but may be due to the properties of specific hydrophobic regions of the carrier as reported for SARS-CoV membrane protein [30]. On SDS-PAGE the wild-type protein ran as three bands at ~55 kDa, ~47.2 kDa and ~35.1 kDa. The three independent approaches used to assess *Hs*PCFT glycosylation status yielded a deglycosylated protein with an apparent molecular size of ~35 kDa, 15 kDa smaller than the predicted size for nonglycosylated *Hs*PCFT (~50 kDa). Further studies using *Hs*PCFT HA tagged on the N- and C-termini excluded the possibility that this discrepancy is due to degradation of the protein. This anomalous electrophoretic behaviour is quite common among polytopic membrane proteins and is similar to what has been reported for the human norepinephrine [31] and glycine transporters [32]. This could be due to (i) the highly hydrophobic nature and basic pI of the transporter [33] and/or, (ii) preservation of the native, compact conformation and decreased SDS binding due to the heating limitation resulting in incomplete denaturation of the *Hs*PCFT protein [34,35]. Decreased SDS binding may decrease the migration rate by reducing the net charge; alternatively, it may increase the migration rate by reducing the mass and frictional drag. The intact disulfide bonds, which usually result in less SDS binding of a more compact shaped protein, can also cause faster migration rates [36]. However, there was no difference in the *Hs*PCFT migration pattern when membranes were prepared with or without DTT before loading onto the gel. Replacement of the seven native cysteine residues with serines had no effect on *Hs*PCFT function;

hence, disulfide bonds are not required for proper HsPCFT folding and function (Unal ES et al., unpublished).

Glycosylation on asparagine 58 and 68 confirms that the first methionine is the actual translation initiation site since the second methionine in the amino acid sequence of *Hs*PCFT is at the 75th position after the glycosylation consensus sites. The results suggest that an approximately 20 kDa oligosaccharide chain is added to *Hs*PCFT when expressed in HeLa cells based upon the size of glycosylated *Hs*PCFT (~55 kDa) and deglycosylated transporters (~35 kDa). It is of interest that *Hs*PCFT may be glycosylated to a different extent in different cells. Hence, ~60 kDa and ~78 kDa size *Hs*PCFT proteins were detected in HepG2 cells and *Xenopus* oocytes, respectively [8]. Further studies on the glycosylation status of *Hs*PCFT from native tissues, and their effect on the migration pattern relative to what is observed in Hela cells, will be of interest.

Similar to most membrane transporters that are N-linked glycosylated on a single large extracellular loop [37], post-translational modification of *Hs*PCFT by N-linked glycosylation at N58 and N68 requires the extracellular localization of this domain, since oligosaccharide chains are transferred *en bloc* from a dolichol donor to the nascent polypeptide simultaneously with translation *only* if the NXS/T consensus site faces the endoplasmic reticulum lumen [38]. This is consistent with a topological model in which the N-terminus is localized to the cytoplasm. This configuration was supported by immunocytochemical analysis of both wild-type and deglycosylated *Hs*PCFT constructs HA tagged at the amino terminus, visualized at the plasma membrane only when cells were first permeabilized with Triton X100 [39–42]. This data also supports a model in which there is an even number of transmembrane domains, requiring that the C-terminus is also localized to the cytoplasm. Hence, wild-type and deglycosylated *Hs*PCFT, HA tagged at the C-terminus, could only be detected after membrane permeabilization.

N-linked glycosylation is not essential for cell surface trafficking and function of RFC [43] and the creatine transporter [44]. On the other hand, N-linked glycosylation can play a role in proper folding of the polypeptide chain, protection from proteolytic degradation [45], maintenance of protein solubility [46] and targeting to subcellular compartments and to the cell surface [47]. The latter role of glycosylation has been reported for many transporters such as the human norepinephrine [31], glycine (GLYT1) [32], glucose (GLUT1) [48], organic anion (OAT4) [47] and organic cation transporters [49]. In these cases the transport proteins are heavily glycosylated on three or more asparagine residues and the deglycosylated protein retains only a small percentage of wild-type activity. In contrast, *Hs*PCFT is glycosylated only on asparagine 58 and 68 and the majority of *Hs*PCFT transport function was preserved in the N58Q/N68Q-*Hs*PCFT mutant. Indeed, the small decrease observed could be due to the amino acid changes per se rather than the absence of glycosyl moieties since, at a tunicamycin concentration sufficient to completely abolish glycosylation, no significant decrease in *Hs*PCFT function could be detected.

N-linked glycosylation scanning mutagenesis is a useful technique to analyze the topology of various transporters [32,50]. The prerequisite for this approach is a functional deglycosylated transporter [51]. The observation that the majority of function is preserved in deglycosylated *Hs*PCFT indicates that glycosylation scanning mutagenesis can be used to further evaluate the secondary structure of this carrier and that bacterial systems can be used to produce large quantities of this transporter for structural studies.

Acknowledgement

This work was supported by a grant from the National Institutes of Health (CA-082621).

References

[1] J. Selhub, G.J. Dhar, I.H. Rosenberg, Gastrointestinal absorption of folates and antifolates, Pharmacol. Ther. 20 (1983) 397–418.
[2] C.H. Halsted, The intestinal absorption of folates, Am J. Clin Nutr. 32 (1979) 846–855.
[3] A.M. Reisenauer, C.H. Halsted, Human jejunal brush border folate conjugase. Characteristics and inhibition by salicylazosulfapyridine, Biochim. Biophys. Acta. 659 (1981) 62–69.
[4] Y. Wang, R. Zhao, R.G. Russell, I.D. Goldman, Localization of the murine reduced folate carrier as assessed by immunohistochemical analysis, Biochim. Biophys. Acta 1513 (2001) 49–54.
[5] H.M. Said, F.K. Ghishan, R. Redha, Folate transport by human intestinal brush-border membrane vesicles, Am. J. Physiol 252 (1987) G229–G236.
[6] C.K. Kumar, T.T. Nguyen, F.B. Gonzales, H.M. Said, Comparison of intestinal folate carrier clone expressed in IEC-6 cells and in *Xenopus* oocytes, Am. J. Physiol 274 (1998) C289–C294.
[7] L.H. Matherly, D.I. Goldman, Membrane transport of folates, Vitam. Horm. 66 (2003) 403–456.
[8] A. Qiu, M. Jansen, A. Sakaris, S.H. Min, S. Chattopadhyay, E. Tsai, C. Sandoval, R. Zhao, M.H. Akabas, I.D. Goldman, Identification of an intestinal folate transporter and the molecular basis for hereditary folate malabsorption, Cell 127 (2006) 917–928.
[9] R. Zhao, S.H. Min, A. Qiu, A. Sakaris, G.L. Goldberg, C. Sandoval, J.J. Malatack, D.S. Rosenblatt, I.D. Goldman, The spectrum of mutations in the PCFT gene, coding for an intestinal folate transporter, that are the basis for hereditary folate malabsorption, Blood. 110 (2007) 1147–1152.
[10] J. Geller, D. Kronn, S. Jayabose, C. Sandoval, Hereditary folate malabsorption: family report and review of the literature, Medicine (Baltimore). 81 (2002) 51–68.
[11] J. Selhub, I.H. Rosenberg, Folate transport in isolated brush border membrane vesicles from rat intestine, J. Biol. Chem. 256 (1981) 4489–4493.
[12] D.W. Horne, Transport of folates and antifolates in liver, Proc. Soc. Exp. Biol. Med. 202 (1993) 385–391.
[13] S.D. Bhandari, S.K. Joshi, K.E. McMartin, Folate binding and transport by rat kidney brush-border membrane vesicles, Biochim. Biophys. Acta 937 (1988) 211–218.
[14] R. Zhao, F. Gao, M. Hanscom, I.D. Goldman, A prominent low-pH methotrexate transport activity in human solid tumor cells: contribution to the preservation of methotrexate pharmacological activity in HeLa cells lacking the reduced folate carrier, Clin. Cancer Res. 10 (2004) 718–727.
[15] S. Chattopadhyay, R. Zhao, S.A. Krupenko, N. Krupenko, I.D. Goldman, The inverse relationship between reduced folate carrier function and pemetrexed activity in a human colon cancer cell line, Mol. Cancer Ther. 5 (2006) 438–449.
[16] R. Zhao, I.D. Goldman, The molecular identity and characterization of a proton-coupled folate transporter—PCFT; biological ramifications and impact on the activity of pemetrexed, Cancer Metastasis Rev. 26 (2007) 129–139.
[17] Y. Wang, R. Zhao, I.D. Goldman, Characterization of a folate transporter in HeLa cells with a low pH optimum and high affinity for pemetrexed distinct from the reduced folate carrier, Clin. Cancer Res. 10 (2004) 6256–6264.
[18] S. Ben Dor, N. Esterman, E. Rubin, N. Sharon, Biases and complex patterns in the residues flanking protein *N*-glycosylation sites, Glycobiology. 14 (2004) 95–101.
[19] L. Kasturi, H. Chen, S.H. Shakin-Eshleman, Regulation of N-linked core glycosylation: use of a site-directed mutagenesis approach to identify Asn-Xaa-Ser/Thr sequons that are poor oligosaccharide acceptors, Biochem. J. 323 (1997) 415–419.
[20] D.W. Fry, J.C. Yalowich, I.D. Goldman, Rapid formation of poly-gamma-glutamyl derivatives of methotrexate and their association with dihydrofolate reductase as assessed by high pressure liquid chromatography in the Ehrlich ascites tumor cell *in vitro*, J. Biol. Chem. 257 (1982) 1890–1896.
[21] K.A. Sharif, I.D. Goldman, Rapid determination of membrane transport parameters in adherent cells, BioTechniques 28 (2000) 926–928, 930, 932.
[22] U.K. Laemmli, Cleavage of structural proteins during the assembly of the head of bacteriophage T4, Nature 227 (1970) 680–685.
[23] N. Quandt, A. Stindl, U. Keller, Sodium dodecyl sulfate-polyacrylamide gel electrophoresis for M(r) estimations of high-molecular-weight polypeptides, Anal. Biochem. 214 (1993) 490–494.
[24] L. Garcia-Ortega, I.R. De, V.A. Martinez-Ruiz, M. Onaderra, J. Lacadena, d.P. Martinez, J.G. Gavilanes, Anomalous electrophoretic behavior of a very acidic protein: ribonuclease U2, Electrophoresis. 26 (2005) 3407–3413.
[25] G.D. Barsomian, T.L. Johnson, M. Borowski, J. Denman, J.F. Ollington, S. Hirani, D.S. McNeilly, J.R. Rasmussen, Cloning and expression of peptide-N4-(*N*-acetyl-beta-D-glucosaminyl)asparagine amidase F in *Escherichia coli*, J. Biol. Chem. 265 (1990) 6967–6972.
[26] T. Tai, K. Yamashita, M. Ogata-Arakawa, N. Koide, T. Muramatsu, S. Iwashita, Y. Inoue, A. Kobata, Structural studies of two ovalbumin glycopeptides in relation to the endo-beta-*N*-acetylglucosaminidase specificity, J. Biol. Chem. 250 (1975) 8569–8575.
[27] A.D. Elbein, Inhibitors of the biosynthesis and processing of N-linked oligosaccharide chains, Annu. Rev. Biochem. 56 (497–534) (1987) 497–534.
[28] M. Shayeghi, G.O. Latunde-Dada, J.S. Oakhill, A.H. Laftah, K. Takeuchi, N. Halliday, Y. Khan, A. Warley, F.E. McCann, R.C. Hider, D.M. Frazer, G.J. Anderson, C.D. Vulpe, R.J. Simpson, A.T. McKie, Identification of an intestinal heme transporter, Cell. 122 (2005) 789–801.
[29] Y. Nakai, K. Inoue, N. Abe, M. Hatakeyama, K.Y. Ohta, M. Otagiri, Y. Hayashi, H. Yuasa, Functional characterization of human PCFT/HCP1 heterologously expressed in mammalian cells as a folate transporter, J. Pharmacol. Exp. Ther. (2007).
[30] Y.N. Lee, L.K. Chen, H.C. Ma, H.H. Yang, H.P. Li, S.Y. Lo, Thermal aggregation of SARS-CoV membrane protein, J. Virol. Methods. 129 (2005) 152–161.
[31] H.E. Melikian, J.K. McDonald, H. Gu, G. Rudnick, K.R. Moore, R.D. Blakely, Human norepinephrine transporter. Biosynthetic studies using a site-directed polyclonal antibody, J. Biol. Chem. 269 (1994) 12290–12297.
[32] L. Olivares, C. Aragon, C. Gimenez, F. Zafra, Analysis of the transmembrane topology of the glycine transporter GLYT1, J. Biol. Chem. 272 (1997) 1211–1217.
[33] A.K. Dunker, R.R. Rueckert, Observations on molecular weight determinations on polyacrylamide gel, J. Biol. Chem. 244 (1969) 5074–5080.

[34] J.S. Tung, C.A. Knight, Relative importance of some factors affecting the electrophoretic migration of proteins in sodium dodecyl sulfate-polyacrylamide gels, Anal. Biochem. 48 (1972) 153–163.
[35] H. Furthmayr, R. Timpl, Characterization of collagen peptides by sodium dodecylsulfate-polyacrylamide electrophoresis, Anal. Biochem. 41 (1971) 510–516.
[36] J.A. Reynolds, C. Tanford, The gross conformation of protein–sodium dodecyl sulfate complexes, J. Biol. Chem. 245 (1970) 5161–5165.
[37] C. Landolt-Marticorena, R.A. Reithmeier, Asparagine-linked oligosaccharides are localized to single extracytosolic segments in multi-span membrane glycoproteins, Biochem. J. 302 (1994) 253–260.
[38] R. Kornfeld, S. Kornfeld, Assembly of asparagine-linked oligosaccharides, Annu. Rev. Biochem. 54 (631–64) (1985) 631–664.
[39] P.L. Ferguson, W.F. Flintoff, Topological and functional analysis of the human reduced folate carrier by hemagglutinin epitope insertion, J. Biol. Chem. 274 (1999) 16269–16278.
[40] J. Geyer, B. Doring, K. Meerkamp, B. Ugele, N. Bakhiya, C.F. Fernandes, J.R. Godoy, H. Glatt, E. Petzinger, Cloning and functional characterization of human sodium-dependent organic anion transporter (SLC10A6), J. Biol. Chem. 282 (2007) 19728–19741.
[41] M. Hong, K. Tanaka, Z. Pan, J. Ma, G. You, Determination of the external loops and the cellular orientation of the N- and the C-termini of the human organic anion transporter hOAT1, Biochem. J. 401 (2007) 515–520.
[42] O. Levy, G. Dai, C. Riedel, C.S. Ginter, E.M. Paul, A.N. Lebowitz, N. Carrasco, Characterization of the thyroid Na+/I− symporter with an anti-COOH terminus antibody, Proc. Natl. Acad. Sci. U. S. A. 94 (1997) 5568–5573.
[43] S.C. Wong, L. Zhang, S.A. Proefke, L.H. Matherly, Effects of the loss of capacity for *N*-glycosylation on the transport activity and cellular localization of the human reduced folate carrier, Biochim. Biophys. Acta 1375 (1998) 6–12.
[44] N. Straumann, A. Wind, T. Leuenberger, T. Wallimann, Effects of N-linked glycosylation on the creatine transporter, Biochem. J. 393 (2006) 459–469.
[45] S.M. Hurtley, D.G. Bole, H. Hoover-Litty, A. Helenius, C.S. Copeland, Interactions of misfolded influenza virus hemagglutinin with binding protein (BiP), J. Cell Biol. 108 (1989) 2117–2126.
[46] P.J. Gallagher, J.M. Henneberry, J.F. Sambrook, M.J. Gething, Glycosylation requirements for intracellular transport and function of the hemagglutinin of influenza virus, J. Virol. 66 (1992) 7136–7145.
[47] F. Zhou, W. Xu, M. Hong, Z. Pan, P.J. Sinko, J. Ma, G. You, The role of N-linked glycosylation in protein folding, membrane targeting, and substrate binding of human organic anion transporter hOAT4, Mol. Pharmacol. 67 (2005) 868–876.
[48] T. Asano, H. Katagiri, K. Takata, J.L. Lin, H. Ishihara, K. Inukai, K. Tsukuda, M. Kikuchi, H. Hirano, Y. Yazaki, The role of *N*-glycosylation of GLUT1 for glucose transport activity, J. Biol. Chem. 266 (1991) 24632–24636.
[49] R.J. Ott, A.C. Hui, K.M. Giacomini, Inhibition of N-linked glycosylation affects organic cation transport across the brush border membrane of opossum kidney (OK) cells, J. Biol. Chem. 267 (1992) 133–139.
[50] X. Liu, L. Matherly, Analysis of membrane topology of the human reduced folate carrier protein by hemagglutinin epitope insertion and scanning glycosylation insertion mutagenesis, Biochim. Biophys. Acta 1564 (2002) 333–342.
[51] M. van Geest, J.S. Lolkema, Membrane topology and insertion of membrane proteins: search for topogenic signals, Microbiol. Mol. Biol. Rev. 64 (2000) 13–33.